http://dx.doi.org/10.7494/miag.2017.4.532.72

ŁUKASZ HEREZY
WALDEMAR KORZENIOWSKI
KRZYSZTOF SKRZYPKOWSKI

Main objectives underlying mathematical model of powered support unit operation in terms of its working capacity

This study synthesizes the operating data of a longwall system to determine the impacts of time, compressive strength of roof rock strata, rate of face advance, and distance between the cross bar in a roof support from the side wall on the value of the actual working capacity of powered supports. The analyses of the general linear models are supported by the Statistica program. Criteria imposed on the input data lead to the development of models of the powered support unit (shield) operation yielding corrected value of the coefficient R2(0,11-0,42), rendering the models statistically significant. For the investigated longwall panel, the minimal bearing capacity of the powered support obtained by several methods is compared with the actual bearing capacity of the powered support units. Mathematical models were recalled to obtain the pressure value that can be used in the further procedure as:

- *pressure in a shield leg required to obtain the load-bearing capacity of a hydraulic leg in response to the load applied to the powered support,*
- *pressure exerted by rock strata on the longwall excavation, which is utilized to determine the real load acting on the powered support unit.*

In the context of these two objectives, the roof stability factor was obtained accordingly, revealing excellent support-strata interactions under the specified geological and mining conditions.

Key words: *operating pressure, bearing capacity, longwall mining method, rock mass pressure*

1. INTRODUCTION

The longwall mining system is one of the most-popular methods of coal extraction world-wide. When compared to the second-best mining method (the room and pillar system), it offers higher productivity; however, the mining machinery and equipment are very costly. The mining machinery and equipment referred to as the longwall system include a shearer (or the coal plow head and its drives), a face conveyor, a drag conveyor, powered supports, an instrumentation truck, and a hydraulic power-supply system. Selecting the longwall system components such that they operate and interact smoothly under the specified geological and mining conditions should guarantee the uninterrupted mining operations and pre-determined output levels [1, 2]. The fundamental criteria in the selection of mining machines include the extraction height (height of the coal seam) as well as the longitudinal and lateral inclination of the longwall site. When the longwall system components have been originally designed to interact, checking this aspect of their performance is not necessary. However, when the machines and longwall equipment are provided by several manufacturers or include components from different mining systems (even if they are provided by one manufacturer), the actual feasibility of machine interactions has to be first ascertained.

In the next step, the production capacity of the coal mining machine and hauling capacity of the face conveyor are checked in the context of ensuring the daily output levels. As regards the powered supports, of particular importance are the technical conditions and shield-strata interactions ensuring roof stability over the working site in the longwall excavation [3, 4, 5, 6, 7, 8–10]. To ensure adequate shield-roof strata interactions, the initial and working capacity of the powered support need to be appropriate [4, 11, 12]. Time-variant working capacity is the response to loading imposed on a powered support by roof strata. Load components contributing the total shield loading include the following [3, 6, 13, 14]:

- rock mass pressure associated with the extraction depth, presence of old excavations, and dip of the coal seam;
- the range of the longwall excavations understood as the distance between the longwall face and caved-in section;
- shield standstill time.

Selecting the powered-support systems and adapting them to the geological and mining conditions does not always guarantee the correct shield-strata interactions. In order that the initial bearing capacity should be uniform and set, the shield legs are equipped with control systems incorporating a secondary pressure-charging system. However, in weak roof zones where a shield has a too-high set pressure (which may contribute to the poorer roof condition), the pressure-charging system is frequently switched off by the operators [12, 15, 16]. Its absence leads to non-uniform leg pressure and, in certain cases, to the inadequate clamping of the shield against the roof, which as a consequence results in roof and wall sliding, the caving-in of the roof rocks, and overloading the powered support units.

2. METHODS OF PARAMETER SELECTION AND TESTING SHIELD-STRATA INTERACTIONS

Most Polish collieries rely on the admissible roof deformation method when assessing the adequacy of shield-roof strata interactions [6, 13, 14].

The condition for adequate roof support is satisfied as long as the value of roof-stability factor g is at least 0.8. It is a critical level; when g is less than 0.8, there is a risk of roof rock sliding and the deterioration of roof conditions. It is a widely accepted view that, for $0.7 = g < 0.8$, there is a risk of roof control problems at longwall sites. These difficulties are associated with the risk of roof strata sliding and the vertical displacement of rock strata [5].

Roof stability factor g is derived from the following formula [6]:

$$g = \frac{1}{\frac{0.65 \cdot z_1}{z_g} + 0.3} \tag{1}$$

where:

z_1 – unit roof inclination,
z_g – critical roof inclination.

Exceeding the critical subsidence value may result in the unravelling of the rock strata. The critical value of the subsidence varies depending on the rock type. Observations at longwall sites have allowed us to find the critical inclination of the roof composed of specific rocks. When exceeded, the roof becomes a loose conglomerate of rock fragments. This quantity is expressed as roof inclination z_g in millimeters per 1 m of roof span [5]:

$$z_g = \frac{k_e}{\frac{0.05}{R_{cs}} + 0.006} \quad \left[\frac{\text{mm}}{\text{m}}\right] \tag{2}$$

where:

k_e – coefficient related to the adopted mining system (0.8 – for caving-in; 0.35 – for hydraulic back-filling),
R_{cs} – compressive strength of roof strata [MPa].

Unit roof inclination z_1 [mm/m], or the roof inclination over the first meter of the excavation range from the longwall face, is the major determinant of roof subsidence over the entire longwall site.

In the case of longwall mining with caving-in, z_1 is derived from the following formula [6]:

$$z_1 = \frac{1}{0.013\, m_p + 0.002} \quad \left[\frac{\text{mm}}{\text{m}}\right] \tag{3}$$

where m_p is the ratio of shield-bearing capacity moment M_p [MN·m] to the moment of the load acting on the excavation M_Q [MN·m].

To determine the unit roof inclination, it is required that resultant bearing capacity moment M_p and the average bearing capacity of powered support P_z should first be calculated (Formula (4)). The average bearing capacity is determined for the face section in which one powered support is set against the roof with the initial bearing capacity, the second powered support is displaced towards the side wall, while the next support unit has not yet been moved. These are the least-favorable conditions experienced during the normal duty cycle of the powered support operation [6]:

$$P_z = \frac{i \cdot n_k \cdot n_w \cdot P_r}{3b} \cdot \left[\frac{(1-n_0)\cdot(d_{02}-d_{01})}{\frac{100 \cdot e^{-3.5 \cdot e^{-8 \cdot n_{cz}}}}{z_{śr}} + \left(1 + e^{-1.8 \cdot e^{-2 \cdot n_{cz}}}\right)} + 2 \cdot n_m \cdot n_0 \right] \text{ [MN]} \quad (4)$$

where:

- i – number of hydraulic legs in the shields,
- n_k – leg capacity reduction factor,
- n_w – factor expressing the bearing capacity transferred from the shield onto the roof,
- P_r – working capacity of shield legs [MN],
- n_o – initial to working capacity ratio,

$$n_o = \frac{P_w}{P_r} \quad (5)$$

- P_w – initial capacity of shield legs [MN],
- d_{02}–d_{01} – initial and final distance of the considered segment of the working to the face,
- n_{cz} – shield performance factor,
- $z_{śr}$ – average convergence of the longwall working over the distance d_{01}–d_{02},
- n_m – factor expressing the impacts of low bearing capacity of surrounding strata.

Moment of shield bearing capacity is expressed as follows [6]:

$$M_p = P_z \cdot l_z \quad [\text{MN·m}] \quad (6)$$

where l_z is the arm length of load-bearing force P_z.

The weight of the rock strata on the longwall site is equal to the weight of a rock mass solid section one meter in width counted alongside the face; its base length normal to the face line and equal to the extent of the longwall excavation. The height of the solid section and the actual shape of side walls are dependent on the adopted extraction method and roof strength.

The load per running meter of the longwall excavation for the longwall mining system with cave-in is expressed as follows [6]:

$$Q = n_q \cdot n_a \cdot h_s \cdot c_w \frac{L_i^{1.4}}{0.13 \cdot R_c^{0.5} + 0.7} \quad [\text{MN}] \quad (7)$$

where:

- n_a – load rate factor,
- n_g – de-stressed strata range factor,
- c_w – bulk density of roof rock [NM/m^3],
- h_s – reduced height of the longwall working [m],
- L_i – longwall site span [m],
- R_c – compressive strength of roof strata [MPa].

The loading moment acting on the longwall excavation is given as follows [6]:

$$M_Q = 0.7 \cdot L_i \cdot Q \quad [\text{MN·m}] \quad (8)$$

The minimal working capacity of a powered support can be derived from the following formula:

$$P = \frac{Q}{0.7}(g - 0.3) \quad [\text{MN}] \quad (9)$$

To guarantee good roof stability, the value of g should be equal to or greater than 0.8.

In countries with a well-established extractive sector and extensive mining expertise, methods have been developed to support the selection of shield capacity.

For example, in Great Britain [17], the minimal bearing capacity of a powered support is derived from the following formula:

$$P \geq \frac{m}{k-1} \cdot \gamma \quad \left[\frac{\text{Mg}}{\text{m}^2}\right] \quad (10)$$

The minimal bearing capacity of powered supports under the geological and mining conditions outlined in Section 3 has been calculated by the presented methods. These results are summarized in Table 1.

Table 1

Minimal shield capacity obtained by selected methods

Lp.	Method	Minimal shield capacity P_{min} [kN/m^2]
1	Poland [17]	200
3	Great Britain [17]	267
4	Germany [17]	214
5	Terzaghi [11]	128
6	Yehia [18]	95

3. GEOLOGICAL AND MINING CONDITIONS

The panel considered in this study was nearly horizontal, the longitudinal inclination angle of the opening-up cross-cut was 2°, and the seam thickness varied from 1.33 m to 1.8 m (with the average value being 1.6 m). The compressive strength of the coal beds fell to within a range of 12–18 MPa. The longwall face to be operated upon was 250 m in length with a 1750-meter range.

The immediate roof in the area was comprised of claystone, mudstone, and sandstone strata. The thickness of the claystone directly above the coal seam ranged from 0.8 m to 2.0 m, revealing the local occurrence of spherical siderite features. Directly overlying the claystone was the mudstone bed; its thickness ranging from 0.2 m to more than 7 m. The mudstone layer was the thickest in the central part of the face range. Overlying the mudstone was a sandstone bed of up to 7 m in thickness (also revealing mudstone interlayers). The sandstone bed was the thickest in the front sections of the face range. Overlying the sandstone bed were alternating layers of claystone, mudstone, and coal. The geomechanical test data yielded a contour map of compressive strength distribution R_c of the roof strata overlying the longwall panel (Fig. 1).

In the floor strata alongside the face range, there was a claystone bed of between 0.3 m to 1.5 m in thickness. Underneath are the alternating mudstone, stigmaria mudstone, sandstone, and claystone strata with coal inclusions, revealing the presence of numerous spherical siderite features (particularly in the mudstone). No faulting or seismic discontinuities were observed in the area. The operated automated plow system incorporated the following components:

- Gliding plow GH 1600 operating at 0.98–2.2 m seam height. The longwall operations use the version with the lowest plow body height (980–1230 m).
- Face conveyor PF-1032 with a front discharge chute.
- Gate-end conveyor PF-1132.
- One hundred and forty-one powered support units. From the gateway end, there are 3 units in the opening section, a linear array of 134 units, and 4 units from the ancillary drive end.

The technical parameters of the powered support sections are summarized in Table 2.

Table 2

Operating parameters of powered support (shield) sections

Parameter		Value	Unit
Shield height range		0.95–2.0	[m]
Operating range		1.0–1.9	[m]
Admissible inclination	longitudinal	to 15°	[–]
	lateral	±15°	[–]
Pitch		1.75	[m]
Step		to 0.85	[m]
Number of legs		2	[pieces]
Leg diameter		Ø320	[mm]
Bearing capacity of the leg	initial (32 MPa)	2573	[MN]
	operating (45 MPa)	3619	[MN]
Cross bar length		4030	[mm]
Operating pressure		45	[MPa]
Supply pressure		32	[MPa]

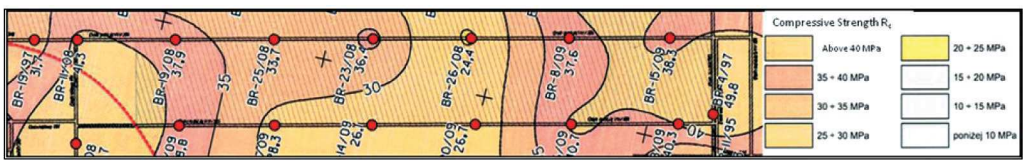

Fig 1. Compressive strength Rc of roof strata up to 6 m above coal seam roof (derived by A. Ruchel)

4. DATA ANALYSIS FROM V-SHIELD PROGRAM

In the considered longwall site roof, support is provided by 141 powered support units. State-of-the-art equipment enables the effective monitoring and visualization of the shield operation as well as control of the remaining machinery within the longwall system. Key parameters obtained from the visualization system include the following [2, 18, 20, 21]:

- p – pressure in the space beneath the piston in the shield leg, [MPa],
- w – length of the divider cylinder in its forth position [m],
- v – rate of face advance [m/day],
- t_p – shield standstill time [min].

The analyses rely on roof baring parameter d m, understood as the distance between the cross-bar end (counting from the face front) and the face, substituted for the length of the divider cylinder in its forth position. Distance d is the component of distance L_t between the cross-beam end and the longwall face (resulting from the actual configuration of the longwall system prior to the cut) and web of coal z. For the longwall system considered in this study, distance L_t is 0.5 m, and the maximal web of coal is taken to be 0.7 m. Maximal roof baring value d should be 1.2 m (though it in fact approached 1.4 m).

Based on the results summarized in [2, 18, 20], for the analyses used:

- powered support units from 30 to 100;
- maximal standstill time t_p below 250 min; within this time period, the shield operates within the working pressure range;
- maximal pressure level 42 MPa;
- minimal pressure level 24 MPa.

It appears that 41% of the roof baring values fall within a range of 0.5 m to 0.6 m (see Fig. 2). Roof baring rates within a range of 0.6 m to 0.9 m follow a similar pattern (44.8%). The remaining interval of roof baring values from the nominal coal web of 1.2 m accounts for 13.6% of the cases. In only 0.5% of the cases, the actual value of d should exceed 1.2 m. Figure 3 illustrates leg pressure distribution p. It appears that, for the pressure increment of 8 MPa (from 24 MPa to 32 MPa), we get 57% of the pressure readings; the remaining 43% are registered following a further pressure increase by 10 MPa (from 32 MPa to 42 MPa). Dominating rates of face advance accounting for 34% of the registered values are those within a range of 10–12 m daily (Fig. 4). The shield standstill time t_p distribution follows a similar pattern (Fig. 5). It appears that, 38% of the registered standstill times are below 10 min, 60% of the registered standstill times coincide with time required to complete the full web of coal (z = 0.7 m), which is equal to 27 min. The remaining 40% of the registered standstill time values are associated with roof baring in excess of 1.2 m.

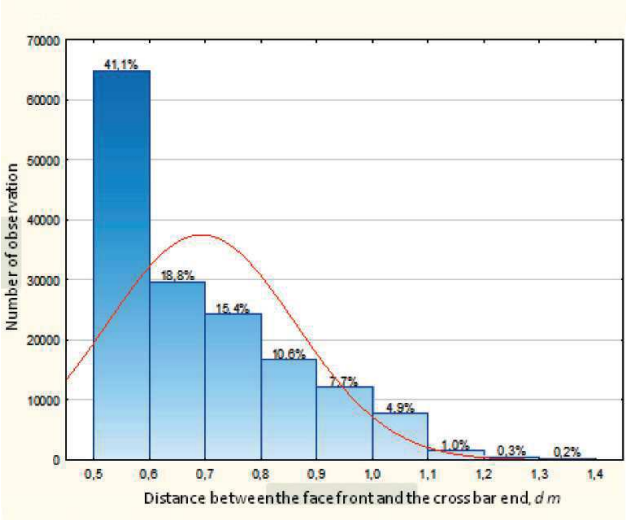

Fig. 2. Roof baring distribution [d]

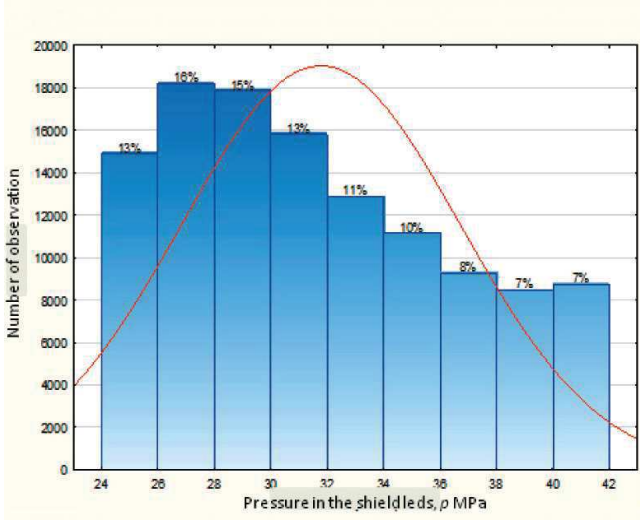

Fig. 3. Distribution of shield leg pressure [p]

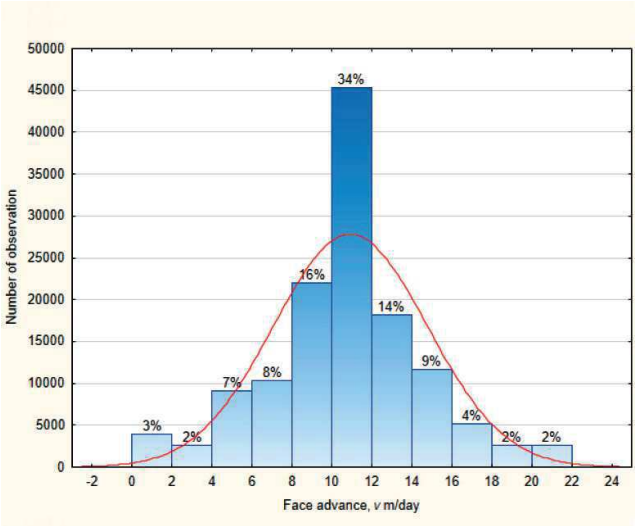

Fig. 4. Distribution of rate of face advance [v]

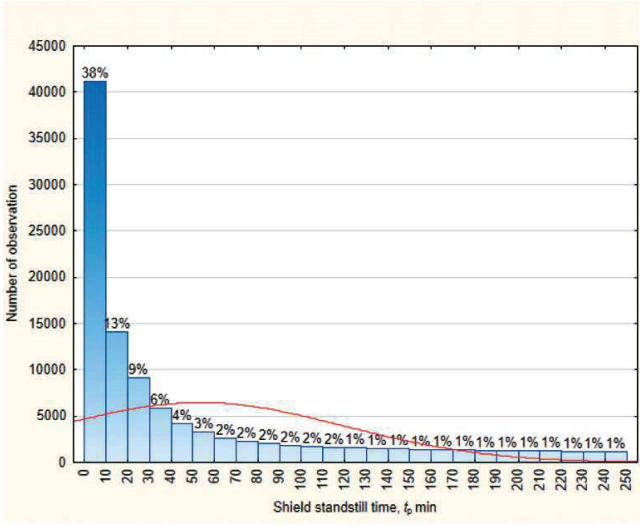

Fig. 5. Shield standstill time [tp]

5. MULTI-PARAMETRIC MODEL OF THE SHIELD OPERATION

The model of the shield performance is based on a linear model that is widely employed in analyses of ANOVA or MANOVA systems incorporating categorized predictors, any ANOVA or MANOVA systems incorporating both categorized and continuous variables, and multiple and multi-dimensional regression models involving continuous independent variables. The model encapsulates two methods of data coding and analysis; interpretation of the measurement data is supported by a model with sigma constraints adapted by Statistica (qualitative predictor coding), which can handle two arbitrary yet different values of single dependent variables (predictors). Thus, the obtained values of the independent variable will represent the group membership in quantitative terms. Typically, the values corresponding to group membership are not selected at random but in a manner supporting the interpretation of the regression coefficient value related to the dependent variable (predictor). In one of the strategies in widespread use, events from two groups are ascribed values of dependent variables equal to 1 and –1; therefore, when the regression coefficient for the given variable is positive, the predicted value of the group encoded in the independent variable as 1 shall be higher (a higher group mean value). When the coefficient of regression is negative, the group encoded in the independent variable as –1 shall produce a higher predicted value of the dependent variable. Another advantage of this approach is that each group is encoded by a value different from zero by one, which makes easier the interpretation of the predicted differences between groups as coefficients of the regression yield; a unit variation of the dependent variable for each unit variation of the independent variable (predictor). This coding strategy is referred to as a parameterization with sigma constraints, because the sets of parameters indicating group membership (1 and –1) sum to zero [22].

Several variants have been considered in the calculation procedure, subdividing the standstill times and roof baring rates in various configurations. The values of the statistical indicators are optimal for the following configuration of operational parameters (Tab. 3):

- standstill time within a range of 0 min to 250 min;
- roof baring process subdivided into intervals:
  - 0.5 m $\leq d <$ 0.6 m,
  - 0.6 m $\leq d <$ 0.9 m,
  - 0.9 m $\leq d <$ 1.2 m,
  - 1.2 m $\leq d <$ 1.4 m.

For barred roof area intervals 0.5 m $\leq d <$ 0.6 m and 1.2 m $\leq d <$ 1.4 m, the rate of face advance is found to be statistically insignificant.

The analysis of the full models revealed their statistical significance, and the corrected value of coefficient R^2 is regarded as satisfactory (Table 4).

Table 3

Statistical significance of model parameters

Effect	Leg pressure, p [MPa]	Leg pressure, p [MPa]	Leg pressure, p [MPa]	Leg pressure, p [MPa]	–95.00 [%]	+95.00 [%]	Leg pressure, p [MPa]	Leg pressure, p [MPa]	–95.00 [%]	+95.00 [%]
Parameter evaluation: sigma parameterization with constraints Acceptance condition: $d \geq 0{,}5$ m; $d < 0{,}6$ m; $p \geq 24$ MPa; $p \leq 42$ MPa; $t_p \leq 250$ min										
Free term	42.271	0.471	89.661	0.000	41.347	43.195				
Roof barring factor	–20.618	0.792	–26.043	0.000	–22.170	–19.066	–0.118	0.005	–0.127	–0.109
Rate of face advance factor	**–0.010**	**0.005**	**–1.888**	**0.059**	**–0.020**	**0.000**	**–0.009**	**0.005**	**–0.018**	**0.000**
Compressive strength of roof strata factor	–0.095	0.005	–17.914	0.000	–0.105	–0.084	–0.081	0.005	–0.090	–0.072
Standstill time of a support unit factor	0.037	0.000	132.103	0.000	0.036	0.037	0.621	0.005	0.611	0.630
Acceptance condition: $d \geq 0.6$ m; $d < 0.9$ m; $p \geq 24$ MPa; $p \leq 42$ MPa; $t_p \leq 250$ min										
Free term	25.763	0.190	135.863	0.000	25.391	26.134				
Roof barring factor	8.577	0.183	46.769	0.000	8.217	8.936	0.176	0.004	0.168	0.183
Rate of face advance factor	–0.032	0.004	–7.286	0.000	–0.041	–0.024	–0.028	0.004	–0.035	–0.020
Compressive strength of roof strata factor	–0.098	0.004	–24.839	0.000	–0.106	–0.090	–0.093	0.004	–0.101	–0.086
Standstill time of a support unit factor	0.038	0.000	138.473	0.000	0.037	0.038	0.528	0.004	0.521	0.536
Acceptance condition: $d \geq 0.9$ m; $d < 1.2$ m; $p \geq 24$ MPa; $p \leq 42$ MPa; $t_p \leq 250$ min										
Free term	28.286	0.546	51.834	0.000	27.216	29.355				
Roof barring factor	7.417	0.477	15.555	0.000	6.483	8.352	0.112	0.007	0.098	0.126
Rate of face advance factor	0.086	0.009	9.336	0.000	0.068	0.104	0.068	0.007	0.054	0.083
Compressive strength of roof strata factor	–0.159	0.008	–20.954	0.000	–0.174	–0.144	–0.152	0.007	–0.166	–0.138
Standstill time of a support unit factor	0.030	0.001	41.595	0.000	0.028	0.031	0.303	0.007	0.289	0.317
Acceptance condition: $d \geq 1.2$ m; $d < 1.4$ m; $p \geq 24$ MPa; $p \leq 42$ MPa; $t_p \leq 250$ min										
Free term	28.459	4.737	6.008	0.000	19.156	37.763				
Roof barring factor	9.302	3.671	2.534	0.012	2.092	16.512	0.100	0.039	0.022	0.177
Rate of face advance factor	**0.075**	**0.048**	**1.589**	**0.113**	**–0.018**	**0.169**	**0.062**	**0.039**	**–0.015**	**0.140**
Compressive strength of roof strata factor	–0.236	0.038	–6.139	0.000	–0.311	–0.160	–0.243	0.040	–0.320	–0.165
Standstill time of a support unit factor	0.030	0.005	5.672	0.000	0.019	0.040	0.221	0.039	0.145	0.298

Table 4

Statistical significance of models

Depend. variable	Multiple R	Multiple R^2	Corrected R^2	SS Model	df Model	MS Model	SS Model	Df Model	MS Model	F	p
Pressure in the shield legs. p [MPa]	SS Test for the full model with respect to SS for the residues Acceptance condition: $d \geq 0.5$ m; $d < 0.6$ m; $p \geq 24$ MPa; $p \leq 42$ MPa; $t_p \leq 250$ min										
	0.65	0.42	0.42	242836.6	4.0	60709.1	331315.4	28241.0	11.73	5174.8	0.0
	Acceptance condition: $d \geq 0.6$ m; $d < 0.9$ m; $p \geq 24$ MPa; $p \leq 42$ MPa; $t_p \leq 250$ min										
	0.57	0.32	0.32	271432.8	4.0	67858.2	575853.8	48471.0	11.88	5711.8	0.0
	Acceptance condition: $d \geq 0.9$ m; $d < 1.2$ m; $p \geq 24$ MPa; $p \leq 42$ MPa; $t_p \leq 250$ min										
	0.36	0.13	0.13	41575.2	4.0	10393.8	283845.8	16852.0	16.84	617.1	0.0
	Acceptance condition: $d \geq 1.2$ m; $d < 1.4$ m; $p \geq 24$ MPa; $p \leq 42$ MPa; $t_p \leq 250$ min										
	0.34	0.12	0.11	1330.1	4.0	332.5	9909.4	582.0	17.03	19.5	0.0

For each analytical procedure, the mathematical model of shield operation is determined accordingly:

The first interval of barred roof area 0.5 m $\leq d <$ 0.6 m is governed by the following formula:

$$p = 42.2711 - 20.6182 \cdot d - 0.0099 \cdot v - 0.0948 \cdot R_c + 0.0369 \cdot t_p \quad [\text{MPa}] \tag{11}$$

The second interval 0.6 m $\leq d <$ 0.9 m is expressed by:

$$p = 25.7626 + 8.5766 \cdot d - 0.0324 \cdot v - 0.0982 \cdot R_c + 0.0375 \cdot t_p \quad [\text{MPa}] \tag{12}$$

Third interval 0.9 m $\leq d <$ 1.2 m is governed by:

$$p = 28.2858 + 7.4174 \cdot d + 0.0857 \cdot v - 0.159 \cdot R_c + 0.0295 \cdot t_p \quad [\text{MPa}] \tag{13}$$

Fourth interval 1.2 m $\leq d <$ 1.4 m is expressed by:

$$p = 28.4591 + 9.3019 \cdot d + 0.0755 \cdot v - 0.2357 \cdot R_c + 0.0296 \cdot t_p \quad [\text{MPa}] \tag{14}$$

6. APPLICATION OF SHIELD OPERATION MODEL TO DETERMINE SHIELD-STRATA INTERACTIONS

Thus, the obtained mathematical models of the shield operations can be used to determine working capacity P_r (Tab. 5) and loading moment M_Q of a powered support as well as roof stability factor g. The predicted values of p derived from Formulas (11)–(14) can be further used in two alternative procedures:

1. Assuming that the predicted value of p is the working capacity of a shield leg P_r (Tab. 5, Column 6), the equivalent bearing capacity P_z (Eq. (4)) and bearing capacity moment M_P (Eq. (6)) can be obtained accordingly. Recalling Equations (7) and (8), we get the loading of the longwall site Q and the loading moment M_Q. These are used to determine roof stability factor g (Eq. (1)). It is readily apparent that the value of g tends to increase with working capacity (Tab. 5, Column 6), indicating good shield-strata interactions. Such a favorable value of g is attributed to the working capacity of a shield leg increasing over time and time-invariant loading of the longwall site.
2. Assuming that the obtained predicted value of p expresses time-variant load Q acting on the longwall excavation, Equation (8) can be recalled to derive loading moment M_Q (Tab. 5, Column 7). The equivalent bearing capacity P_z is determined for nominal values of working capacity P_r and initial capacity P_w of a powered support (Eq. (4)). Shield capacity moment M_p is derived from Equation (6), and roof stability factor g is obtained from Formula (1) (Tab. 5, Column 8). It appears that the values of g are lower by half, which is attributed to the fixed value of working capacity P_r while the load acting on the longwall site Q tends to increase over time. Nevertheless, the obtained values of g are still sufficient to guarantee adequate shield-strata interactions. In this particular case, the value of g tends to decrease with increasing standstill time t_p.

Table 5

Selected values of roof stability factor derived from mathematical models of shield operation

R_c [MPa]	d [m]	v [m/day]	t_p [min]	g	P_r [MN]	M_Q [MNm]	g
1	2	3	4	5	6	7	8
30	0.5	5	30	2.03	2.57	16.29	0.92
		10		2.03	2.57	16.29	0.92
		15		2.03	2.57	16.29	0.92
		20		2.03	2.57	16.29	0.92
		5	60	2.03	2.57	16.29	0.92
		10		2.03	2.57	16.29	0.92
		15		2.03	2.57	16.29	0.92
		20		2.03	2.57	16.29	0.92
		5	250	2.07	3.07	19.46	0.84
		10		2.07	3.07	19.46	0.84
		15		2.07	3.07	19.46	0.84
		20		2.07	3.06	19.40	0.84
30	0.8	5	30	2.00	2.57	17.37	0.95
		10		2.00	2.57	17.37	0.95
		15		2.00	2.57	17.37	0.95
		20		2.00	2.57	17.37	0.95
		5	60	2.00	2.57	17.37	0.95
		10		2.00	2.57	17.37	0.95
		15		2.00	2.57	17.37	0.95
		20		2.00	2.57	17.37	0.95
		5	250	2.05	3.12	21.09	0.85
		10		2.05	3.11	21.02	0.85
		15		2.05	3.10	20.96	0.85
		20		2.05	3.08	20.82	0.86
30	1.1	5	30	1.97	2.65	19.03	0.95
		10		1.98	2.68	19.24	0.95
		15		1.98	2.72	19.53	0.94
		20		1.98	2.75	19.75	0.93
		5	60	1.98	2.72	19.53	0.94
		10		1.98	2.75	19.75	0.93
		15		1.99	2.79	20.03	0.93
		20		1.99	2.82	20.25	0.92
		5	250	2.02	3.17	22.76	0.86
		10		2.02	3.20	22.98	0.86
		15		2.03	3.24	23.26	0.85
		20		2.03	3.27	23.48	0.85

Table 5 cont.

30	1.2	5	30	1.97	2.71	19.84	0.95
		10		1.97	2.74	20.06	0.94
		15		1.97	2.77	20.28	0.94
		20		1.98	2.80	20.50	0.93
		5	60	1.97	2.78	20.35	0.93
		10		1.98	2.81	20.57	0.93
		15		1.98	2.85	20.86	0.92
		20		1.98	2.88	21.08	0.92
		5	250	2.02	3.24	23.72	0.86
		10		2.02	3.27	23.94	0.86
		15		2.02	3.30	24.16	0.85
		20		2.02	3.33	24.32	0.85
30	1.4	5	30	1.96	2.86	21.74	0.93
		10		1.96	2.89	21.96	0.93
		15		1.97	2.92	22.19	0.92
		20		1.97	2.95	22.42	0.92
		5	60	1.97	2.93	22.27	0.92
		10		1.97	2.96	22.50	0.91
		15		1.97	2.99	22.72	0.91
		20		1.97	3.03	23.03	0.90
		5	250	2.01	3.39	25.77	0.85
		10		2.01	3.42	25.99	0.85
		15		2.01	3.45	26.22	0.84
		20		2.02	3.48	26.45	0.84

Despite the major discrepancies between the obtained values of g, the two approaches are both correct (although there are some differences in the way they should be interpreted). In the first approach, we get an indicator of the adequate roof-strata interactions under the fixed roof conditions. The second approach provides information that the load acting on the longwall site is increasing and that the roof--strata interactions tend to deteriorate.

At that stage of research work, it is reasonable to rely on Formulas (11)–(14) to prognosticate the loading Q of the longwall site. However, it can be expected that, in further analyses investigating other longwall faces and various stages of the shield operation, the first approach may prove more useful.

7. CONCLUSIONS

The minimal bearing capacity of a powered support was obtained for the specified geological and mining conditions and for the given longwall equipment. The derived maximal value was 265 kN/m^2, and the minimal value was found to be 95 kN/m^2. The value obtained by the methodology in widespread use in Polish collieries was 200 kN/m^2. The minimal working capacity of the investigated powered support was 720 kN/m^2.

Data collected in the program registering longwall system performance were used in the analysis of the shield operation parameters taking into account the imposed constraints: maximal standstill time t_p

not exceeding 250 min, maximal pressure 42 MPa, and the minimal pressure level 24 MPa.

Statistical analyses reveal that 41% of roof baring values fall within a range of 0.5 m to 0.6 m.

During the standstill time of 60 min, shields were moved towards the longwall face to support the roof, and 40% of the standstill times were registered throughout the analyzed period.

A relatively high number of registered standstill times did not exceed 10 min (38% of the cases).

A pressure increase of 8 MPa is registered in 57% of the cases, and the remaining 43% reveal a pressure increase of 10 MPa. It is reasonable to expect that the pressure distribution in particular pressure intervals follows a similar pattern.

A thorough analysis of the key parameter distributions has prompted the selection of criteria underpinning the shield operation models:

- standstill time within a range of 0 to 250 min;
- roof baring process subdivided into intervals:
  - $0.5\ \text{m} \le d < 0.6\ \text{m}$,
  - $0.6 \le d < 0.9\ \text{m}$,
  - $0.9\ \text{m} \le d < 1.2\ \text{m}$,
  - $1.2\ \text{m} \le d < 1.4\ \text{m}$.

For barred roof area intervals $0.5\ \text{m} \le d < 0.6\ \text{m}$ and $1.2\ \text{m} \le d < 1.4\ \text{m}$, the rate of face advance is found to be statistically insignificant.

Shield operation models taking into account all investigated predictors are found to be statically significant (Tab. 4), and the obtained corrected values of R^2: 0.42. 0.32; 12, 11 are regarded as satisfactory.

Respective models are governed by Equations (11)–(14), yielding a pressure level that can be interpreted as a loading acting on the longwall site Q or the working capacity of the shield leg P_r. On this basis, the values of roof stability factor g are obtained, indicating adequate shield-strata interactions in both cases. The initial and working bearing capacity under the conditions in the investigated longwall panel have been selected to leave a considerable safety margin.

At this stage of research work, the approach relying on shield monitoring data from the longwall panel and interpreting the predicted value of p as load Q acting on the longwall site appears to be more useful.

The results obtained thus far encourage the further development of the research methods and tools used in rock strata monitoring during longwall mining, offering us better insight into shield-strata interactions.

References

[1] Bołoz Ł.: *Unique project of single-cutting head longwall shearer used for thin coal seams exploitation*, "Archives of Mining Sciences" 2013, 58, 4: 1057–1070.

[2] Korzeniowski W., Herezy Ł. Krauze K., Rak Z., Skrzypkowski K.: *Rock mass monitoring based on analysis of powered support response*, Wydawnictwa AGH, Kraków 2013.

[3] Barczak T.M.: *A retrospective assessment of longwall roof support with a focus on challenging accepted roof support concepts and design premises*, 25th International Conference on Ground Control in Mining, Morgantown, West Virginia 2006.

[4] Barczak T.M., Esterhuizen G.S., Ellenberger J., Zahng P.: *A first step in developing standing roof support design criteria based on ground reaction data for Pittsburgh seam longwall tailgate support*, 27th International conference on ground control in mining, Morgantown, West Virginia 2008.

[5] Biliński A.: *Principles of underground working maintenance in longwalls with rockburst hazard*, "Archives of Mining Science" 1983, 28, 2: 275–291.

[6] Biliński A.: *Metoda doboru obudowy ścianowych wyrobisk wybierkowych i chodnikowych do warunków pola eksploatacyjnego*, Prace naukowe – monografie CMG Komag, Gliwice 2005.

[7] Hoyer D.: *Early warning of longwall of cavities using LVA software*, 12th Coal Operators' Conference, University of Wollongong & the Australasian Institute of Mining and Metallurgy, Wollongong 2012.

[8] Trueman R., Lyman G., Cocker A.: *Longwall roof control through a fundamental understanding of shield-strata interaction*, "Journal of Rock Mechanics Mining Science" 2009, 46: 371–380.

[9] Trueman R., Callan M., Thomas R., Hoyer D.: *Quantifying the impact of cover depth and panel width on longwall shield-strata interactions*, 10th Coal Operators Conference, Wollongong 2010.

[10] Trueman R., Thomas R., Hoyer D.: *Understanding the causes of roof control problems on a longwall face from shield monitoring data – a case study*, 11th Underground Coal Operators Conference, University of Wollongong & the Australasian Institute of Mining and Metallurgy, Wollongong 2011.

[11] Mahmoud Y.S.: *Estimation of bearing capacity of power support in front of longwall face*, The Fourth Mining, Petroleum and Metallurgy Conference, Faculty of Engineering, Assiut University, Mining Engineering 1994, 1, 1: 251–255.

[12] Pawlikowski A.: *Wpływ podporności wstępnej na podporność stojaków sekcji obudowy zmechanizowanej*, "Mining – Informatics, Automation and Electrical Engineering" 2016, 4: 72–79.

[13] Płonka M.: *Load variation of the set of support in the longwall with roof caving*, "Research Reports Mining and Environment" 2009, 1: 41–49.

[14] Prusek S., Płonka A., Walentek A.: *Applying the ground reaction curve concept to the assessment of shield support performance in longwall faces*, "Arabian Journal of Geosciences" 2016, 9: 1–15.

[15] Pawlikowski A.: *Przyczyny asymetrii podporności stojaków sekcji obudowy zmechanizowanej w świetle badań dołowych*, "Maszyny Górnicze" 2017, 1: 45–54.

[16] Szyguła M.: *Progress in designing the powered roof support in Poland*, "Maszyny Górnicze" 2013, 2: 30–38.

[17] Cemal B., Ergin A.: *Design of Supports in Mines*, John Wiley & Sons, New York 1983.

[18] Herezy Ł.: *Predicting the vertical convergence of longwall headings basing on the pressure increase factor ξ*, AGH University of Science and Technology, Kraków 2017 [unpublished work].

[19] Hussein M.A., Ibrahim A.R., Imbaby S.S.: *Load calculations and selection of the powered supports based on rock mass classification and other formulae for Abu-Tartur longwall phosphate mining conditions*, "Journal of Engineering Sciences" 2013, 41, 4: 1728–1742.

[20] Herezy Ł.: *Relationship between vertical convergence of longwall headings and the pressure increase factor ξ for a powered support section*, AGH University of Science and Technology, Krakow 2017 [unpublished].

[21] Przegendza G., Przegendza M.: *Control and diagnostics systems for mining machines and equipment using a CAN bus*, "Szybkobieżne Pojazdy Gąsienicowe" 2007, 2: 1–11.

[22] https://www.statsoft.pl/textbook/stathome.html [online], September 2017.

ŁUKASZ HEREZY, Ph.D., Eng.
WALDEMAR KORZENIOWSKI, prof.
KRZYSZTOF SKRZYPKOWSKI, Ph.D., Eng.
Underground Mining Department
Faculty of Mining and Geoengineering
AGH University of Science and Technology
al. Mickiewicza 30, 30-059 Krakow, Poland
{herezy, walkor, skrzypo}@agh.edu.pl